THE JOURNAL OF PHYSICAL CHEMISTRY B

Article

pubs.acs.org/JPCB

Toward Organic Photohydrides: Excited-State Behavior of 10-Methyl-9-phenyl-9,10-dihydroacridine

Xin Yang,[†] Janitha Walpita,[†] Dapeng Zhou,[†] Hoi Ling Luk,[‡] Shubham Vyas,[‡] Rony S. Khnayzer,[†] Subodh C. Tiwari,[§] Kadir Diri,[§] Christopher M. Hadad,[‡] Felix N. Castellano,[†] Anna I. Krylov,[§] and Ksenija D. Glusac*,[†]

[†]Department of Chemistry and Center for Photochemical Sciences, Bowling Green State University, Bowling Green, Ohio 43403, United States

[‡]Department of Chemistry, The Ohio State University, Columbus, Ohio 43210, United States

[§]Department of Chemistry, University of Southern California, Los Angeles, California 90089-0482, United States

Supporting Information

ABSTRACT: The excited-state hydride release from 10-methyl-9-phenyl-9,10-dihydroacridine (PhAcrH) was investigated using steady-state and time-resolved UV/vis absorption spectroscopy. Upon excitation, PhAcrH is oxidized to the corresponding iminium ion ($PhAcr^+$), while the solvent (acetonitrile/water mixture) is reduced (52% of $PhAcr^+$ and 2.5% of hydrogen is formed). The hydride release occurs from the triplet excited state by a stepwise electron/hydrogen-atom transfer mechanism. To facilitate the search for improved organic photohydrides that exhibit a concerted mechanism, a computational methodology is presented that evaluates the thermodynamic parameters for the hydride ion, hydrogen atom, and electron release from organic hydrides.

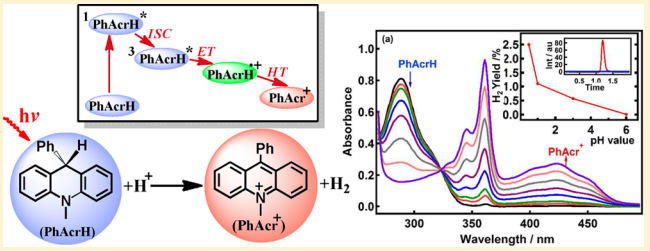

INTRODUCTION

The reduced form of nicotinamide-adenine dinucleotide (NADH) is a biological cofactor that performs hydride transfer reactions to various substrates, and these reactions are driven by the stabilization of the aromatized NAD^+ product.[1] Given its biological significance, the mechanism of hydride transfer from NADH and its analogues has been extensively studied.[2−10] These studies have shown that the overall hydride release occurs either by a concerted single-step process[2−5] or by one of the sequential mechanisms, such as electron−proton−electron[6−9] or electron−hydrogen atom transfers.[2,10] The overall mechanism can be controlled by varying the one-electron reduction potential of the donor and acceptor or the pK_a value of the radical cation of the NADH analogue.[5,11]

If the hydride transfer from the NADH analogue is driven photochemically, the desired reduction of the substrate could be powered using the photon's energy. Such a photochemical event can, in turn, be used to generate solar fuels, by reducing protons to hydrogen[12−18] or carbon dioxide to methanol,[19] via simple earth-abundant organic structures. Motivated by this perspective, we present here a study of the excited-state hydride release from one of the widely used NADH analogues, a dihydroacridine derivative PhAcrH (Scheme 1a). We previously investigated the photochemistry of a hydroxylated analogue (PhAcrOH), which was shown to undergo a fast (τ = 108 ps) release of the hydroxide ion in protic solvents.[20] These results have provided initial evidence that the acridine framework exhibits a tendency to undergo the excited-state heterolytic bond cleavage to generate the aromatic $PhAcr^+$ product upon excitation. In the absence of protic solvation, PhAcrOH exhibited no photochemistry and its excited state decayed to the ground state by an $S_1 \rightarrow T_1 \rightarrow S_0$ sequence of intersystem crossing steps.

This study investigates the hydride transfer from the photoexcited PhAcrH to the solvent (acidified acetonitrile/water mixture). We present steady-state and time-resolved (fs−ns range) UV/vis absorption experiments and the supporting

Scheme 1. Excited State Hydride Release from PhAcrH: (a) the Overall Photochemical Reaction in Acetonitrile and pH 0.65 H_2O Mixture (V:V = 1:1); (b) Proposed Mechanism

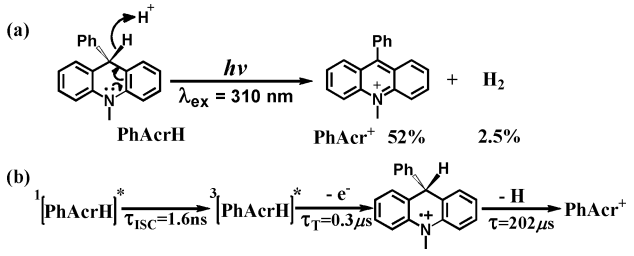

Special Issue: Michael D. Fayer Festschrift

Received: February 19, 2013
Revised: May 4, 2013
Published: May 9, 2013

density functional theory (DFT) calculations showing that the photochemical hydride release indeed occurs from the excited PhAcrH, and that the mechanism involves a sequential e−H transfer process, as shown in Scheme 1b. These results are discussed in terms of thermodynamic driving forces for the excited-state processes.

EXPERIMENTAL SECTION

All chemicals were purchased from commercial suppliers and used without further purification unless otherwise noted. ^{1}H NMR spectra were recorded on a Bruker Avance 300 MHz system. UV/vis absorption spectra were recorded on an Agilent 8453 UV Spectrophotometer in a 1 cm quartz cell. GC analyses were performed by means of a Shimadzu GC-14A gas chromatograph equipped with a TCD column. GC-MS analysis was done with a Shimadzu QP 5050 gas chromatograph mass spectrometer.

Synthesis. PhAcrH(D) was synthesized according to the literature under modified conditions.[7]

10-Methyl-9-phenyl-9,10-dihydroacridine (PhAcrH). $PhAcr^+$ (450 mg, 1.2 mmol) was suspended in 20 mL of ethanol. Sodium borohydride ($NaBH_4$) (90 mg, 2.4 mmol) in ethanol was added dropwise over a period of 5 min. The resulting colorless solution was refluxed for 2 h. Ethanol was evaporated in vacuo at room temperature, and the crude product was extracted with dichloromethane (3 × 40 mL). The organic layer was dried over $CaCl_2$ and recrystallized from ethanol to give PhAcrH as white crystals (276 mg, 85%). ^{1}H-NMR (300 MHz, CD_3CN): 3.38 (s, 3 H), 5.23 (s, 1 H), 6.9−7.3 (m, 13 H).

The deuterated compound (PhAcrD) was prepared by the same procedure with $NaBD_4$ and purified by recrystallization. ^{1}H-NMR (300 MHz, CD_3CN): 3.36 (s, 3 H), 6.8−7.4 (m, 13 H).

Steady State UV/vis Absorption Experiment. Solutions of ∼0.1 mM PhAcrH were prepared in acetonitrile:water (1:1) mixture at different pH values. For oxygen-free experiments, the samples were degassed for 45 min with argon prior to the experiments. For the experiments in the presence of oxygen, the samples were prepared under atmospheric conditions. As the irradiation source, a medium pressure Hg arc lamp (Hanovia PC 451050) was used and the excitation wavelengths were controlled below 350 nm using a short pass filter (Asahi Spectra USA Inc.). All irradiations were performed at room temperature. The conversion of PhAcrH to $PhAcr^+$ was monitored using UV/vis spectrophotometry at different time intervals.

GC Hydrogen Detection. Shimadzu GC-8A was operated with ultrahigh purity argon as carrier gas and a 5 Å molecular sieve column (Restek) to separate gas mixtures. This GC was customized with two injection ports, the first for syringe injections and the second for automatic injections from a 500 μL sample loop directly linked to a Schlenk line. The detector was calibrated against known amounts of H_2 gas. In principle, 500 μL of 10% H_2 balanced Ar certified gas standard (Praxair) was injected at different pressures using a home-built Schlenk line linked to a pressure gauge. The area under the hydrogen peak was then plotted against the calculated number of the moles of hydrogen injected to get the calibration constant of the detector. This constant was then verified by syringe injections of different volumes of 25% H_2 balanced Ar certified gas standard (Praxair), equilibrated to atmospheric pressure and placed in an airtight vial. The calibration was performed routinely with variation typically below 5% at a certain Ar flow rate (Figure S1, Supporting Information). A solution of 0.25 mM PhAcrH in acetonitrile and pH 0.50 water (1:1) mixture was prepared in a custom built quartz reactor capped with a PTFE septum (the solution volume was 54 mL; the headspace volume was 18 mL). After irradiation, a 100 μL sample from the mixture headspace was injected into the GC using a Hamilton airtight syringe and the amount of hydrogen was quantified. The baseline hydrogen detection was done with the exact same conditions and components but in the absence of PhAcrH.

H_2O_2 Detection. Hydrogen peroxide was detected by using the triiodide method.[21] A solution of 0.08 mM PhAcrH was prepared in acetonitrile:water (1:1) mixture and irradiated (vide supra) for 12 min. The irradiated sample was treated with a solution of excess NaI, and the formation of I_3^- was monitored on the basis of UV/vis absorption (λ_{max} at 290 nm = 5.2×10^3).[21]

Femtosecond Transient Absorption Experiment. The 800 nm laser pulses were produced at a 1 kHz repetition rate by a mode-locked Ti:sapphire laser (Hurricane, Spectra-Physics). The output from the Hurricane was split into pump (85%) and probe (10%) beams. The pump beam (800 nm) was sent into an optical parametric amplifier (OPA-800C, Spectra Physics) to obtain 305−310 nm excitation sources. The probe beam was focused into a horizontally moving CaF_2 crystal for white light continuum generation between 350 and 800 nm. The flow cell (Starna Cell Inc. 45-Q-2, 0.9 mL volume with 2 mm path length), pumped by a Fluid Metering RHSY Lab pump (Scientific Support Inc.), was used to prevent photodegradation of the sample. After passing through the cell, the continuum was coupled into an optical fiber and input into a CCD spectrograph (Ocean Optics, S2000). The data acquisition was achieved using in-house LabView (National Instruments) software routines. The group velocity dispersion of the probing pulse was determined using nonresonant optical Kerr effect (OKE) measurements. Sample solutions were prepared at a concentration needed to have an absorbance of 1.0 at the excitation wavelength.

Nanosecond Transient Absorption Experiment. The nanosecond laser flash photolysis experimental setup utilized for measurements in this paper is described in detail elsewhere.[22] Briefly, a Nd:YAG laser (Spectra Physics LAB-150-10) was used as the excitation source with an excitation wavelength of 266 nm. All of the solutions utilized in these experiments were made such that the absorptivity at 266 nm was 1. Transient absorption spectra were recorded using a Roper ICCD-Max 512T digital intensified CCD camera with up to 2 ns temporal resolution. The single wavelength kinetic measurements were recorded using a PMT connected to an oscilloscope, which was directly connected to a computer that runs a custom LabView control and acquisition program.

Computational Methods. All thermochemical calculations were performed using the wB97X-D functional.[23,24] The solvation free energies were computed using the CPCM model.[25] Excited-state calculations were performed using TDDFT/TDA with various functionals. All calculations were performed using the Q-Chem electronic structure package.[26] Additional information is available in section 7b of the Supporting Information.

dx.doi.org/10.1021/jp401770e | J. Phys. Chem. B 2013, 117, 15290−15296

RESULTS AND DISCUSSION

The photochemical behavior of PhAcrH is affected by the molecular oxygen and by the pH of the solution. In the presence of oxygen, efficient photooxidation of PhAcrH to $PhAcr^+$ was observed using UV/vis absorption spectroscopy (Figure S2, Supporting Information), and similar results were reported previously for acridine[27−30] and other NADH derivatives.[31−33] While H_2O_2 is the likely coproduct in this reaction, the iodide test detected only minor amounts of H_2O_2 (Figure S2c, Supporting Information), possibly due to the reaction of PhAcrH with triiodide (Supporting Information).[34] In the absence of oxygen and at neutral pH, photooxidation of PhAcrH to $PhAcr^+$ did not occur. Instead, other photoproducts are formed (Figure S3, Supporting Information), possibly dimers formed upon bimolecular coupling of PhAcr radicals formed upon irradiation (Figure S3, Supporting Information).[35]

Importantly, a decrease of the solution pH in the absence of oxygen leads to the formation of increasing amounts of $PhAcr^+$ (Figure S4, Supporting Information). Figure 1a shows an

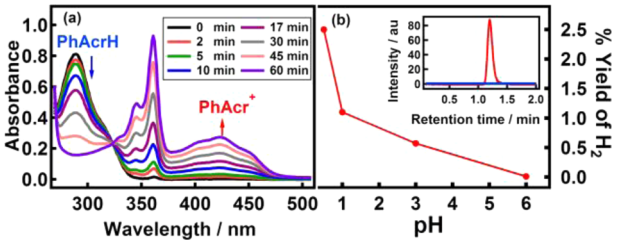

Figure 1. Photoirradiation of 0.1 mM PhAcrH in ACN and pH 0.65 H_2O mixture (V:V = 1:1), in the absence of O_2, λ_{exc} = 220−350 nm. (a) UV/vis absorption changes upon irradiation. (b) Yield percentage of H_2, detected using GC as a function of pH. (The inset in part b shows the GC signals for H_2 in the absence (blue) and in the presence (red) of 0.25 mM PhAcrH.)

example of such behavior recorded at pH 0.65, showing that 52% of $PhAcr^+$ is formed at the end of photoirradiation. Head space analysis via gas chromatography of the irradiated solution shows that the hydrogen is formed in this process, as one would expect for the photoreduction of water by PhAcrH. However, the quantitative analysis revealed that the yield of hydrogen relative to the starting PhAcrH is only 2.5% at pH 0.65 (Figure 1b), suggesting that the photoreduction by PhAcrH involves mostly reduction of the cosolvent acetonitrile, possibly generating protonated ethyl amine, which is known to be formed upon reduction of acetonitrile either chemically by molecular hydrogen and hydrides[36] or electrochemically.[37] Unfortunately, the measurements could not be achieved in purely aqueous solution, due to the low solubility of PhAcrH in water. Our attempts to replace acetonitrile with other cosolvents, such as tetrahydrofuran, were not successful (the irradiation of the sample generated >50% hydrogen, but the PhAcrH converted to a product that was not $PhAcr^+$). This setback can most likely be avoided in the future by the use of water-soluble photohydrides.

To investigate the mechanism of photoreduction by PhAcrH, femtosecond and nanosecond UV/vis transient absorption experiments were collected. The initially formed transient is assigned to the singlet excited state of PhAcrH and exhibits a broad absorption in the visible range (brown spectrum in Figure 2a). The S_1 state exhibits a two-component decay with lifetimes of τ_1 = 26 ps and τ_2 = 1.6 ns (Figure 2b). The origin of

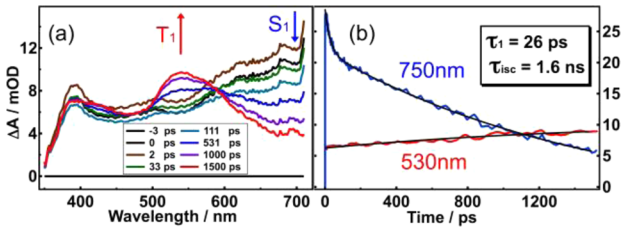

Figure 2. (a) Femtosecond transient absorption spectra of 1 mM PhAcrH in ACN and pH 0.65 H_2O mixture (V:V = 1:1). (b) Kinetics at λ_{exc} = 310 nm.

the 26 ps lifetime is currently not known; it is likely due to the solvation dynamics of PhAcrH in the excited state. The 1.6 ns decay is accompanied by a growth of the new transient with λ_{max} = 550 nm (2.25 eV). A similar species was observed in transient absorption spectra of PhAcrOH in aprotic solvation[20] and was assigned to the triplet excited state. The intersystem crossing (τ = 1.6 ns for PhAcrH and 1.4 ns for PhAcrOH[20]) is faster than expected for a molecule that lacks heavy atoms. However, similar findings were reported previously, where the relatively fast intersystem crossing was explained by transitions between states with different electronic configurations (El-Sayed rule).[38] It is likely that the similar mechanism operates in the case of PhAcrH.

Additional support for the assignment of the 550 nm (2.25 eV) intermediate to the T_1 state of PhAcrH is provided by time-dependent density functional theory (TD-DFT) calculations (Figure S6, Supporting Information). The computed maximum in the T_1 absorption spectrum is at 2.13 eV, which is slightly red-shifted (by 0.12 eV) relative to the experimental maximum. This is within error bars of the theoretical method employed, as confirmed by the differences between computed and observed absorption maxima of other species (Table 1). These results provide additional support for the assignment of the 550 nm band to the T_1 state of PhAcrH.

Table 1. Positions of the First Peak (eV/nm) in the Calculated and Experimental Spectra of Different PhAcrH Species

	position of the first peak (eV/nm)		
	calculation	experiment	difference
PhAcrH(cis2)	4.62/268	4.29/289	0.33
$PhAcr^+$	3.20/388	2.91/426	0.29
$PhAcr^•$	2.74/453	2.48/500	0.26
$PhAcrH^{•+}$	2.26/549	1.89/655	0.37
^{3}[PhAcrH]*	2.13/583	2.25/550	0.12

In addition to the formation of the T_1 state at 550 nm, another transient is formed at 430 nm (2.88 eV). The formation of this intermediate competes with intersystem crossing and is pH-dependent. Femtosecond transient absorption spectra of PhAcrH in ACN:water mixtures were obtained at several pH values (Figure 3). At pH 7, the initially formed S_1 state decays with a concurrent formation of an intermediate with absorption at 550 nm, which is assigned to the T_1 state of PhAcrH. As the solution pH is lowered, another process competes with intersystem crossing. This process leads to a decrease in the absorption at 550 nm and the formation of a new transient with absorption in the 420−440 nm range. The possibility of excited-state protonation of the PhAcrH S_1 state

dx.doi.org/10.1021/jp401770e | J. Phys. Chem. B 2013, 117, 15290−15296

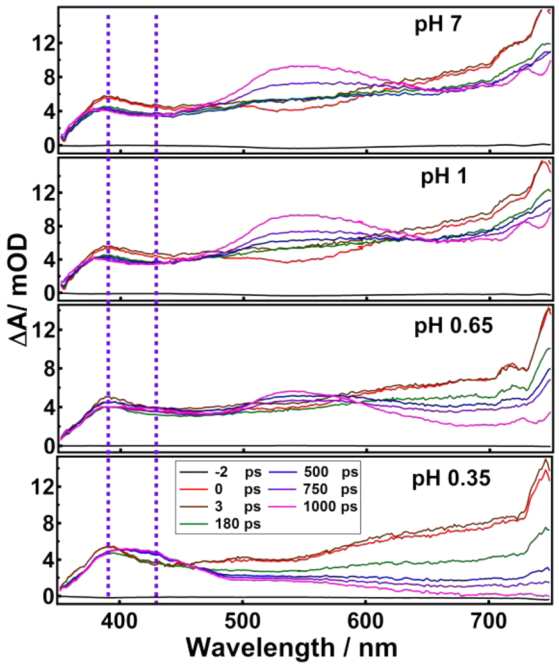

Figure 3. Femtosecond transient absorption spectra of 1 mM PhAcrH in ACN:H_2O (1:1) mixture (the water pH was varied as shown). λ_{exc} = 310 nm.

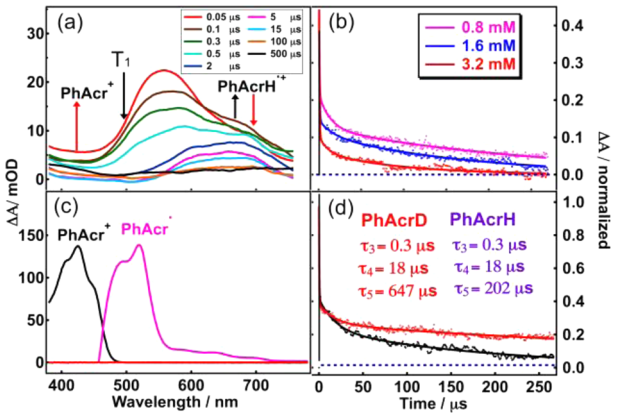

Figure 4. (a) Nanosecond transient absorption spectra of 0.18 mM PhAcrH in ACN and pH 0.65 H_2O mixture (V:V = 1:1), in the absence of O_2, λ_{exc} = 266 nm. (b) Kinetics of different concentrations of PhAcrH in ACN and pH 0.65 H_2O mixture (V:V = 1:1) at 580 nm: 0.8 mM (pink), 1.6 mM (blue), 3.2 mM (red). (c) UV/vis absorption spectrum of 1 mM $PhAcr^+$ (black) and PhAcr radical (pink) in ACN. (d) Kinetics of PhAcrH(D) in ACN and pH 0.65 H_2O mixture (V:V = 1:1) at 580 nm.

was excluded, since TD-DFT calculations predict the absorption of protonated ground-state $PhAcrH_2^+$ to appear at 254 nm, which is below the spectral range covered in our transient absorption experiment. In addition, the formation of protonated $PhAcrH_2^+$ in the S_1 state was not considered, since the 420−440 nm intermediate exhibits a lifetime longer than 1 μs. We postulate that this intermediate is an excimer of PhAcrH, consistent with the previous studies of excimers formed from aromatic compounds.[39,40] The PhAcrH excimer eventually decays to the ground monomeric state, and no photochemical hydride release occurs via this pathway.

The T_1 state of PhAcrH transfers an electron to the solvent with a τ_3 = 0.3 μs lifetime (Figure 4d and Figure S5, Supporting Information) to generate $PhAcrH^{\bullet+}$, with its characteristic absorption in the 500−800 nm range.[6,7] The dynamics of $PhAcrH^{\bullet+}$ exhibit two components: (i) decay with a τ_4 = 18 μs lifetime, possibly due to the electron recombination to generate PhAcrH in the ground state; (ii) decay with τ_5 = 202 μs, which is assigned to the transfer of a hydrogen atom to generate an iminium ion $PhAcr^+$. The assignment of this decay to the H-atom transfer is based on the following findings: (i) the $PhAcrH^{\bullet+}$ decay is coupled with the growth of a band at 425 nm (Figure 4a), which is assigned to $PhAcr^+$ (absorbs at 425 nm, black spectrum in Figure 4c); (ii) the deprotonation of $PhAcrH^{\bullet+}$ was not observed; the deprotonation is expected to generate neutral $PhAcr^{\bullet}$ radical with its absorption band at 500 nm (purple spectrum in Figure 4c),[20] which was not detected in the transient absorption spectrum of PhAcrH (Figure 4a); (iii) the kinetic isotope effect was observed for the lifetime τ_3 when deuterated PhAcrD sample was investigated (Figure 4d), with $k_H/k_D \sim 3$ (the value is a rough estimate, since the time scale of the experiment is insufficient for accurate determinations of these rate constants). The presence of the kinetic isotope effect is indicative of a hydrogen-atom transfer process.[2,41]

The acceptor of the hydrogen atom released from $PhAcrH^+$ is either the solvent or another molecule of $PhAcrH^+$. To determine the nature of the accepting species, the kinetics of $PhAcrH^+$ were investigated as a function of PhAcrH concentration. The lifetime τ_3 of $PhAcrH^+$ at 580 nm decreases as the PhAcrH concentration increases, as shown in Figure 4b (the lifetime decreases from 264 μs at low concentrations to 93 μs at high concentration). This behavior is indicative of a bimolecular process, in which the overall hydrogen atom from $PhAcrH^+$ is released by an electron transfer to another $PhAcrH^+$ coupled with a release of the proton to the solvent (second equation presented below). On the basis of these experimental findings, we propose that the photochemical oxidation of PhAcrH to $PhAcr^+$ occurs in the following sequence of steps:

$$^1[PhAcrH]^* \rightarrow {}^3[PhAcrH]^* \qquad (k_{isc} = 0.63\ ns^{-1})$$

$$^3[PhAcrH]^* \rightarrow PhAcrH^{\bullet+} + e^- \qquad (k_{ET} = 3.3\ \mu s^{-1})$$

$$2PhAcrH^{\bullet+} \rightarrow PhAcr^+ + PhAcrH + H^+$$

$$5H^+ + 4e^- + CH_3CN \rightarrow CH_3CH_2NH_3^+$$

$$2H^+ + 2e^- \rightarrow H_2$$

It is interesting to compare the photochemical behavior of PhAcrH with the previously reported photochemistry of PhAcrOH.[20] Despite similar electronic structures, the S_1 state of PhAcrOH releases OH^- in a single fast step, while PhAcrH releases hydride ion from its T_1 state by a two-step mechanism. To evaluate the driving force for each of these photochemical events, we employ a simple Förster cycle,[42] which is frequently applied to evaluations of excited-state acidities of aromatic alcohols.[43] Using the excitation energies of PhAcrH/PhAcrOH and $PhAcr^+$, as well as evaluated ΔG values for the corresponding ground-state reactions, one finds that the Gibbs free energy change for the excited state release of OH^- ion from PhAcrOH is ΔG_{OH}^* = −24.2 kcal/mol, while this value is ΔG_H^* = −13.7 kcal/mol for the one-step proton reduction by excited PhAcrH (Scheme 2 and section 7a in the

dx.doi.org/10.1021/jp401770e | J. Phys. Chem. B 2013, 117, 15290−15296

Scheme 2. Gibbs Free Energy Profile for Photochemical Processes of PhAcrH in the Presence of a Proton in Aqueous Solution

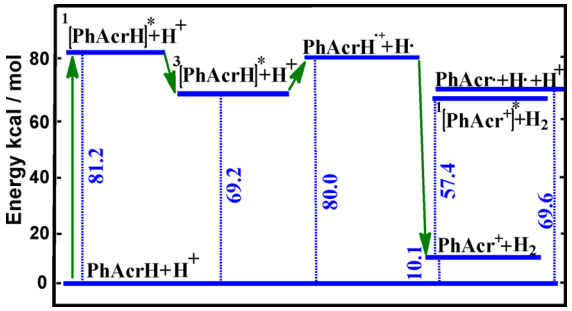

Supporting Information). This breakdown shows that the simple Förster cycle cannot be used to explain the difference in the photochemical behavior of PhAcrOH and PhAcrH: both processes are thermodynamically favored, while only the concerted hydroxide release from excited PhAcrOH was observed experimentally. In contrast, the one-step proton reduction to hydrogen by excited PhAcrH does not occur; instead, the reaction proceeds via electron transfer followed by H-atom transfer. The difference in behavior between PhAcrOH and PhAcrH likely arises due to different barriers for the two photochemical processes. In the case of PhAcrOH, the hydrogen bonding between the −OH group of PhAcrOH and the protic solvent (methanol) facilitates the heterolytic C−OH bond cleavage. The lack of such interaction between the C−H group of PhAcrH and the solvent makes the one-step hydride transfer less likely to occur. Scheme 2 presents energies for different photochemical pathways of PhAcrH estimated from published electrochemical measurements in aqueous solution[44−47] (more detail is available in section 7a, Supporting Information). It is interesting to note that the hydrogen formation from PhAcrH in the ground state is slightly uphill, by only 10.1 kcal/mol. This result suggests that the excitation by UV photon provides much more energy than is required for this process and that, in theory, this process could be driven by low-energy red photons. We note that the driving force for the electron release from the T_1 state of PhAcrH presented in Scheme 2 suggests that this process is not thermodynamically favorable, even though we observe the formation of the PhAcrH$^{\bullet+}$ in the experiment. Two possible explanations are suggested for this discrepancy: (i) the derivation of thermodynamic parameters was performed using aqueous solvation, while the actual experiment was performed in the acetonitrile:water mixture; this solvent mixture possibly alters the ΔG values reported in Scheme 2; (ii) it is possible that the radical cation is formed before the T_1 state is populated, possibly from the T_2 state of PhAcrH.

Hydride release via stepwise mechanisms is not desirable for the following reasons: (i) the radicals generated after each step are reactive and can undergo unwanted chemistry; (ii) the stepwise processes are more energy-demanding, making it unlikely to drive such photochemistry using low-energy visible photons. Thus, it is advantageous to tune the electronic properties of organic hydride donors to enable the concerted process. The first step toward this goal is the development of chemical systems that exhibits thermodynamically favorable excited-state reduction of protons, while the ΔG values for the excited-state electron and hydrogen-atom transfer should be positive. While this thermodynamic condition does not ensure that the photoreduction will take place, it does increase its likelihood. Computational methods are a useful tool to screen model systems, where the calculated thermodynamic parameters for the proton reduction can be obtained from the following calculated quantities: (i) one-electron oxidation potentials of organic hydrides; (ii) Gibbs free energy for the release of a hydride ion from the organic hydride in solution (i.e., PhAcrH → PhAcr$^+$ + H$^-$); (iii) Gibbs free energy for the release of a hydrogen atom from the organic hydride in solution (i.e., PhAcrH → PhAcr$^\bullet$ + H$^\bullet$); (iv) excitation energies of the organic hydride and the corresponding iminium cation.

To facilitate the search for photohydrides that act via a concerted mechanism, we developed a computational protocol that allows us to evaluate the driving forces for hydride ion, hydrogen atom, and electron release from organic hydrides (section 7b, Supporting Information). In our approach, the gas-phase electronic energy differences are evaluated by wB97X-D/6-311(+,+)G(2df,p)[23,24] and thermodynamic corrections at the wB97X-d/6-31+G(d,p) level of theory, while the solvation energetics for all species except hydride ion were evaluated using the CPCM model.[25] Due to computational challenges associated with the solvation energy for the hydride ion,[48] this value was obtained using the experimental reduction potential for the H/H$^-$ couple and the appropriate thermodynamic cycle.[49] The resulting value is ΔG_{solv} = −68.265 kcal/mol. Using this energy, we arrive to the absolute free energy of hydride in acetonitrile G_{abs}(H$^-$/ACN) = −402.9 kcal/mol. This is quite far (9.8 kcal/mol off) from the recently reported value (−412.7 kcal/mol).[48] However, it is close to another reported value (−404.7 kcal/mol)[50,51] (section 7b3, Supporting Information). Additional corrections due to deficiencies in calculated solvation energies of cationic species[52] and spin contamination were made using model compound $AcrH_2$ as an "internal reference"[53] (section 7b4, Supporting Information). Using this approach, the ΔG values for hydride ion, hydrogen atom, and electron release from PhAcrH were evaluated, as presented in Table 2. The calculated values are in excellent agreement with the experimental energies, suggesting that this approach can be used for the computational screening of a large series of organic hydrides. Time-dependent computational methods can then be used to evaluate the excited-state energetics and spectroscopic properties of reaction intermediates.

Table 2. Gibbs Free Energy for Electron, Proton, and Hydrogen Transfer Processes of PhAcrH in Acetonitrile

	ΔG (kcal/mol)		
	PhAcrH$^{\bullet+}$ + e$^-$	PhAcr$^+$ + H$^-$	PhAcr$^\bullet$ + H$^\bullet$
experiment	126.1	76.3	69.6
calculation	126.3	74.1	67.9

CONCLUSIONS

This manuscript describes a study of the photochemical hydride release from an organic hydride, PhAcrH. Using time-resolved spectroscopy, we find that the hydride release occurs via a stepwise electron-hydrogen atom transfer process. The photo-induced concerted hydride transfer was not observed, even though it is thermodynamically favored. To facilitate the search for organic photohydrides that can undergo a concerted hydride release, we developed a computational methodology for evaluation of the relevant thermodynamic parameters.

dx.doi.org/10.1021/jp401770e | J. Phys. Chem. B 2013, 117, 15290−15296

■ ASSOCIATED CONTENT

Supporting Information

Experimental procedures, computational methodology, TA laser setup, supplementary figures, and results. This material is available free of charge via the Internet at http://pubs.acs.org.

■ AUTHOR INFORMATION

Corresponding Author

*E-mail: kglusac@bgsu.edu.

Notes

The authors declare no competing financial interest.

■ ACKNOWLEDGMENTS

This work was supported by National Science Foundation (CHE-1055397 CAREER award to K.D.G.). A.I.K. acknowledges support from the Department of Energy through the DE-FGO2-05ER15685 grant and from the Humboldt Foundation (Bessel Research Award). R.S.K. was supported by a McMaster Fellowship.

■ REFERENCES

(1) Nicotinamide-adenine-dinucleotide. *Concise Encyclo-pedia Biochemistry*, 2nd ed.; Walter de Gruyer: New York, 1988.

(2) Zhu, X. Q.; Liu, Y. C.; Cheng, J. P. Which Hydrogen Atom Is First Transferred in the NAD(P)H Model Hantzsch Ester Mediated Reactions via One-Step and Multistep Hydride Transfer? *J. Org. Chem.* **1999**, *64*, 8980−8981.

(3) Zhu, X. Q.; Zou, H. L.; Yuan, P. W.; Liu, Y.; Cao, L.; Cheng, J. P. A Detailed Investigation into the Oxidation Mechanism of Hantzsch 1,4-Dihydropyridines by Ethyl α-Cyanocinnamates and Benzylidene-malononitriles. *J. Chem. Soc., Perkin Trans. 2* **2000**, 1857−1861.

(4) Simon, J.; Guimarães, C. R. W.; Corréa, M. B.; de Oliveira, C. A. F.; da Cunha Pinto, A.; de Alencastro, R. B. Synthetic and Theoretical Studies on the Reduction of Electron Withdrawing Group Conjugated Olefins Using the Hantzsch 1,4-Dihydropyridine Ester. *J. Org. Chem.* **2003**, *68*, 8815−8822.

(5) Coleman, C. A.; Rose, J. G.; Murray, C. J. General Acid Catalysis of the Reduction of p-Benzoquinone by an NADH Analog. Evidence for Concerted Hydride and Hydron Transfer. *J. Am. Chem. Soc.* **1992**, *114*, 9755−9762.

(6) Fukuzumi, S.; Kotani, H.; Lee, Y. M.; Nam, W. Sequential Electron-Transfer and Proton-Transfer Pathways in Hydride-Transfer Reactions from Dihydronicotinamide Adenine Dinucleotide Analogues to Non-Heme Oxoiron (IV) Complexes and p-Chloranil. Detection of Radical Cations of NADH Analogues in Acid-Promoted Hydride-Transfer Reactions. *J. Am. Chem. Soc.* **2008**, *130*, 15134−15142.

(7) Fukuzumi, S.; Tokuda, Y.; Kitano, T.; Okamoto, T.; Otera, J. Electron-Transfer Oxidation of 9-Substituted 10-Methyl-9,10-Dihydroacridines. Cleavage of the Carbon-Hydrogen vs. Carbon-Carbon Bond of the Radical Cations. *J. Am. Chem. Soc.* **1993**, *115*, 8960−8968.

(8) Miller, L. L.; Valentine, J. R. On the Electron-Proton-Electron Mechanism for 1-Benzyl-1,4-dihydronicotinamide Oxidations. *J. Am. Chem. Soc.* **1988**, *110*, 3982−3989.

(9) Fukuzumi, S.; Suenobu, T.; Patz, M.; Hirasaka, T.; Itoh, S.; Fujitsuka, M.; Ito, O. Selective One-Electron and Two-Electron Reduction of C_{60} with NADH and NAD Dimer Analogues via Photoinduced Electron Transfer. *J. Am. Chem. Soc.* **1998**, *120*, 8060−8068.

(10) Andrew, T. L.; Swager, T. M. A Fluorescence Turn-On Mechanism to Detect High Explosives RDX and PETN. *J. Am. Chem. Soc.* **2007**, *129*, 7254−7255.

(11) Yuasa, J.; Fukuzumi, S. A Mechanistic Dichotomy in Concerted *versus* Stepwise Pathways in Hydride and Hydrogen Transfer Reactions of NADH Analogues. *J. Phys. Org. Chem.* **2008**, *21*, 886−896.

(12) Heyduk, A. F.; Nocera, D. G. Hydrogen Produced from Hydrohalic Acid Solutions by a Two-Electron Mixed-Valence Photocatalyst. *Science* **2001**, *293*, 1639−1641.

(13) White, T. A.; Whitaker, B. N.; Brewer, K. J. Discovering the Balance of Steric and Electronic Factors Needed to Provide a New Structural Motif for Photocatalytic Hydrogen Production from Water. *J. Am. Chem. Soc.* **2011**, *133*, 15332−15334.

(14) McCormick, T. M.; Calitree, B. D.; Orchard, A.; Kraut, N. D.; Bright, F. V.; Detty, M. R.; Eisenberg, R. Reductive Side of Water Splitting in Artificial Photosynthesis: New Homogeneous Photosystems of Great Activity and Mechanistic Insight. *J. Am. Chem. Soc.* **2010**, *132*, 15480−15483.

(15) Curtin, P. N.; Tinker, L. L.; Burgess, C. M.; Cline, E. D.; Bernhard, S. Structure−Activity Correlations among Iridium(III) Photosensitizers in a Robust Water-Reducing System. *Inorg. Chem.* **2009**, *48*, 10498−10506.

(16) Dempsey, J. L.; Brunschwig, B. S.; Winkler, J. R.; Gray, H. B. Hydrogen Evolution Catalyzed by Cobaloximes. *Acc. Chem. Res.* **2009**, *42*, 1995−2004.

(17) Jacques, P. A.; Artero, V.; Pécaut, J.; Fontecave, M. Cobalt and Nickel Diimine-Dioxime Complexes as Molecular Electrocatalysts for Hydrogen Evolution with Low Overvoltages. *Proc. Natl. Acad. Sci. U.S.A.* **2009**, *106*, 20627−20632.

(18) Pool, D. H.; Stewart, M. P.; O'Hagan, M.; Shaw, W. J.; Roberts, J. A. S.; Bullock, R. M.; DuBois, D. L. Calculation of Thermodynamic Hydricities and the Design of Hydride Donors for CO_2 Reduction. *Proc. Natl. Acad. Sci. U.S.A.* **2012**, *109*, 15634−15662.

(19) Morris, A. J.; Meyer, G. J.; Fujita, E. Molecular Approaches to the Photocatalytic Reduction of Carbon Dioxide for Solar Fuels. *Acc. Chem. Res.* **2009**, *42*, 1983−1994.

(20) Zhou, D.; Khatmullin, R.; Walpita, J.; Miller, N. A.; Luk, H. L.; Vyas, S.; Hadad, C. M.; Glusac, K. D. Mechanistic Study of the Photochemical Hydroxide Ion Release from 9-Hydroxy-10-methyl-9-phenyl-9,10-dihydroacridine. *J. Am. Chem. Soc.* **2012**, *134*, 11301−11303.

(21) Fukuzumi, S.; Kuroda, S.; Tanaka, T. Flavin Analog-Metal Ion Complexes Acting as Efficient Photocatalysts in the Oxidation of p-Methylbenzyl Alcohol by Oxygen under Irradiation with Visible Light. *J. Am. Chem. Soc.* **1985**, *107*, 3020−3027.

(22) Shi, X.; Mandel, S. M.; Platz, M. S. On the Mechanism of Reaction of Radicals with Tirapazamine. *J. Am. Chem. Soc.* **2007**, *129*, 4542−4550.

(23) Chai, J. D.; Head-Gordon, M. Systematic Optimization of Long-Range Corrected Hybrid Density Functionals. *J. Chem. Phys.* **2008**, *128*, 084106.

(24) Chai, J. D.; Head-Gordon, M. Long-Range Corrected Hybrid Density Functionals with Damped Atom−Atom Dispersion Corrections. *Phys. Chem. Chem. Phys.* **2008**, *10*, 6615−6620.

(25) Barone, V.; Cossi, M. Quantum Calculation of Molecular Energies and Energy Gradients in Solution by a Conductor Solvent Model. *J. Phys. Chem. A* **1998**, *102*, 1995−2001.

(26) Shao, Y.; Molnar, L. F.; Jung, Y.; Kussmann, J.; Ochsenfeld, C.; Brown, S. T.; Gilbert, A. T. B.; Slipchenko, L. V.; Levchenko, S. V.; O'Neill, D. P. Advances in Methods and Algorithms in a Modern Quantum Chemistry Program Package. *Phys. Chem. Chem. Phys.* **2006**, *8*, 3172−3191.

(27) Fukuzumi, S.; Kondo, Y.; Mochizuki, S.; Tanaka, T. Complex Formation between NADH Model Compounds and Metalloporphyrins. *J. Chem. Soc., Perkin Trans. 2* **1989**, 1753−1761.

(28) Shukla, D.; De Rege, F.; Wan, P.; Johnston, L. J. Laser Flash Photolysis and Product Studies of the Photoionization of N-Methylacridan in Aqueous Solution. *J. Phys. Chem.* **1991**, *95*, 10240−10246.

(29) Fukuzumi, S.; Ishikawa, M.; Tanaka, T. Mechanisms of Photo-Oxidation of NADH Model Compounds by Oxygen. *J. Chem. Soc., Perkin Trans. 2* **1989**, 1037−1045.

(30) Fukuzumi, S.; Yorisue, T. 10,10′-Dimethyl-9,9′-biacridine Acting as a Unique Electron Source Compared with the Corresponding Monomer for the Efficient Reduction of Dioxygen, Catalysed by a

Cobalt Porphyrin in the Presence of Perchloric Acid. *J. Chem. Soc., Perkin Trans. 2* **1991**, 1607−1611.
(31) Fukuzumi, S.; Patz, M.; Suenobu, T.; Kuwahara, Y.; Itoh, S. ESR Spectra of Superoxide Anion−Scandium Complexes Detectable in Fluid Solution. *J. Am. Chem. Soc.* **1999**, *121*, 1605−1606.
(32) Vitinius, U.; Schaffner, K.; Demuth, M.; Heibel, M.; Selbach, H. New Photoproducts from Irradiation of NADH with Near-UV Light. *Chem. Biodiversity* **2004**, *1*, 1487−1497.
(33) Tanaka, M.; Ohkubo, K.; Fukuzumi, S. DNA Cleavage by UVA Irradiation of NADH with Dioxygen via Radical Chain Processes. *J. Phys. Chem. A* **2006**, *110*, 11214−11218.
(34) Fukuzumi, S.; Mochizuki, S.; Tanaka, T. Efficient Catalytic Systems for Electron Transfer from an NADH Model Compound to Dioxygen. *Inorg. Chem.* **1990**, *29*, 653−659.
(35) Anne, A.; Fraoua, S.; Hapiot, P.; Moiroux, J.; Saveant, J. M. Steric and Kinetic Isotope Effects in the Deprotonation of Cation Radicals of NADH Synthetic Analogs. *J. Am. Chem. Soc.* **1995**, *117*, 7412−7421.
(36) Rusik, C.; Collins, M.; Gamble, A.; Tonker, T.; Templeton, J. L. Reactions of η^2-Acyl Ligands in $Tp'(CO)_2Mo[\eta^2\text{-}C(O)R]$ Complexes to Form Complexed Enolates and Enones, Allyls, and Alkyne Insertion Products. *J. Am. Chem. Soc.* **1989**, *111*, 2550−2560.
(37) Huynh, M. H. V.; Meyer, T. J. Proton-Coupled Electron Transfer from Phosphorus: A P−H/P−D Kinetic Isotope Effect of 178. *Angew. Chem., Int. Ed.* **2002**, *41*, 1395−1398.
(38) El-Sayed, M. Spin—Orbit Coupling and the Radiationless Processes in Nitrogen Heterocyclics. *J. Chem. Phys.* **1963**, *38*, 2834−2838.
(39) Katoh, R.; Katoh, E.; Nakashima, N.; Yuuki, M.; Kotani, M. Near-IR Absorption Spectrum of Aromatic Excimers. *J. Phys. Chem. A* **1997**, *101*, 7725−7728.
(40) Benten, H.; Guo, J.; Ohkita, H.; Ito, S.; Yamamoto, M.; Sakumoto, N.; Hori, K.; Tohda, Y.; Tani, K. Intramolecular Singlet and Triplet Excimers of Triply Bridged [3.3.n](3,6,9) Carbazolophanes. *J. Phys. Chem. B* **2007**, *111*, 10905−10914.
(41) Yuasa, J.; Fukuzumi, S. Mechanistic Borderline between One-Step Hydrogen Transfer and Sequential Transfers of Electron and Proton in Reactions of NADH Analogues with Triplet Excited States of Tetrazines and $Ru(bpy)_3^{2+}$*. *J. Am. Chem. Soc.* **2006**, *128*, 14281−14292.
(42) Forster, T. *Z. Elektrochem.* **1950**, *54*, 42−46.
(43) Tolbert, L. M.; Solntsev, K. M. Excited-State Proton Transfer: From Constrained Systems to "Super" Photoacids to Superfast Proton Transfer. *Acc. Chem. Res.* **2002**, *35*, 19−27.
(44) Pavlishchuk, V. V.; Addison, A. W. Conversion Constants for Redox Potentials Measured versus Different Reference Electrodes in Acetonitrile Solutions at 25 °C. *Inorg. Chim. Acta* **2000**, *298*, 97−102.
(45) Isse, A. A.; Gennaro, A. Absolute Potential of the Standard Hydrogen Electrode and the Problem of Interconversion of Potentials in Different Solvents. *J. Phys. Chem. B* **2010**, *114*, 7894−7899.
(46) Handoo, K. L.; Cheng, J. P.; Parker, V. D. Hydride Affinities of Organic Radicals in Solution. A Comparison of Free Radicals and Carbenium Ions as Hydride Ion Acceptors. *J. Am. Chem. Soc.* **1993**, *115*, 5067−5072.
(47) Hapiot, P.; Moiroux, J.; Saveant, J. M. Electrochemistry of $NADH/NAD^+$ Analogs. A Detailed Mechanistic Kinetic and Thermodynamic Analysis of the 10-Methylacridan/10-Methylacridinium Couple in Acetonitrile. *J. Am. Chem. Soc.* **1990**, *112*, 1337−1343.
(48) Muckerman, J. T.; Achord, P.; Creutz, C.; Polyansky, D. E.; Fujita, E. Calculation of Thermodynamic Hydricities and the Design of Hydride Donors for CO_2 Reduction. *Proc. Natl. Acad. Sci. U.S.A.* **2012**, *109*, 15657−15662.
(49) Kelly, C. A.; Rosseinsky, D. R. Estimates of Hydride Ion Stability in Condensed Systems: Energy of Formation and Solvation in Aqueous and Polar-Organic Solvents. *Phys. Chem. Chem. Phys.* **2001**, *3*, 2086−2090.
(50) Kovács, G.; Pápai, I. Hydride Donor Abilities of Cationic Transition Metal Hydrides from DFT-PCM Calculations. *Organometallics* **2006**, *25*, 820−825.
(51) Nimlos, M. R.; Chang, C. H.; Curtis, C. J.; Miedaner, A.; Pilath, H. M.; DuBois, D. L. Calculated Hydride Donor Abilities of Five-Coordinate Transition Metal Hydrides $[HM(diphosphine)_2]^+$ (M= Ni, Pd, Pt) as a Function of the Bite Angle and Twist Angle of Diphosphine Ligands. *Organometallics* **2008**, *27*, 2715−2722.
(52) Sviatenko, L.; Isayev, O.; Gorb, L.; Hill, F.; Leszczynski, J. Toward Robust Computational Electrochemical Predicting the Environmental Fate of Organic Pollutants. *J. Comput. Chem.* **2011**, *32*, 2195−2203.
(53) Konezny, S. J.; Doherty, M. D.; Luca, O. R.; Crabtree, R. H.; Soloveichik, G. L.; Batista, V. S. Reduction of Systematic Uncertainty in DFT Redox Potentials of Transition-Metal Complexes. *J. Phys. Chem. C* **2012**, *116*, 6349−6356.